ACS APPLIED MATERIALS & INTERFACES

Research Article

Cite This: ACS Appl. Mater. Interfaces 2019, 11, 47810−47821

www.acsami.org

Biomimetic Micropatterned Adhesive Surfaces To Mechanobiologically Regulate Placental Trophoblast Fusion

Zhenwei Ma,[†] Lucas Sagrillo-Fagundes,[†,‡,§] Raymond Tran,[†] Prabu Karthick Parameshwar,[∥] Nikita Kalashnikov,[†] Cathy Vaillancourt,[‡,§] and Christopher Moraes*[,†,∥,⊥]

[†]Department of Chemical Engineering, McGill University, Montréal, QC H3A 0C5, Canada

[‡]INRS-Centre Armand Frappier Santé Biotehnologie and Réseau Intersectoriel de Recherche en Santé de l'Université du Québec, Laval, QC H7V 1B7, Canada

[§]Center for Interdisciplinary Research on Well-Being, Health, Society and Environment, Université du Québec à Montréal, Montréal, QC H3C 3P8, Canada

[∥]Department of Biological and Biomedical Engineering, McGill University, Montréal, QC H3A 2B4, Canada

[⊥]Rosalind and Morris Goodman Cancer Research Centre, McGill University, Montréal, QC H3A 1A3, Canada

Supporting Information

ABSTRACT: The placental syncytiotrophoblast is a giant multinucleated cell that forms a tree-like structure and regulates transport between mother and baby during development. It is maintained throughout pregnancy by continuous fusion of trophoblast cells, and disruptions in fusion are associated with considerable adverse health effects including diseases such as preeclampsia. Developing predictive control over cell fusion in culture models is hence of critical importance in placental drug discovery and transport studies, but this can currently be only partially achieved with biochemical factors. Here, we investigate whether biophysical signals associated with budding morphogenesis during development of the placental villous tree can synergistically direct and enhance trophoblast fusion. We use micropatterning techniques to manipulate physical stresses in engineered microtissues and demonstrate that biomimetic geometries simulating budding robustly enhance fusion and alter spatial patterns of synthesis of pregnancy-related hormones. These findings indicate that biophysical signals play a previously unrecognized and significant role in regulating placental fusion and function, in synergy with established soluble signals. More broadly, our studies demonstrate that biomimetic strategies focusing on tissue mechanics can be important approaches to design, build, and test placental tissue cultures for future studies of pregnancy-related drug safety, efficacy, and discovery.

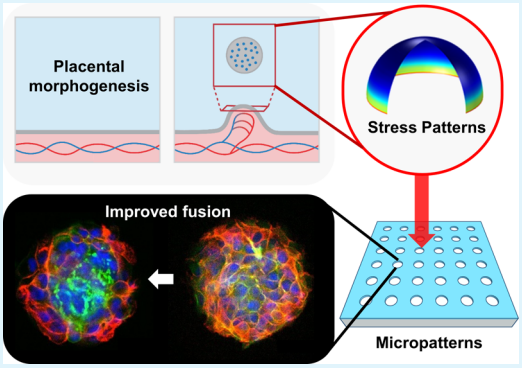

KEYWORDS: *mechanobiology, micropattern, fusion, trophoblast, placenta, biomimetic, development*

INTRODUCTION

In vitro culture models are of critical importance in addressing pregnancy-related diseases as the study of pregnant human females is fraught with ethical, technical, and safety challenges; also, animal models do not adequately capture human reproductive physiology.[1] Given the wide-range and long-term impact of placental dysfunction on our healthcare economy and on patient's quality of life,[2,3] developing practical and realistic strategies for in vitro culture of placental tissue is required to better understand this vital organ.

Fusion of cells into a single multinuclear structure is an important characteristic of several biological processes, including differentiation of bone, muscle, and placental tissues.[4−6] In the placenta, the syncytiotrophoblast (STB) is a giant, fused, polarized, multinucleated cell that covers the villous placental tree on the maternal side (Figure 1A). This complex three-dimensional structure is highly branched[7] and provides sufficient surface area to regulate essential transport of metabolites and waste across the fetal−maternal interface throughout pregnancy.[8] In addition, the STB produces and secretes hormones necessary for maternal physiological adaptation and fetal development[9] and provides resistance to maternal immunological challenges.[10] The formation of a well-defined syncytial sheath over the villous trees is not well conserved across species and accessible animal models,[11] and it is hence challenging to study the factors that drive the initial formation of this critically important syncytial layer during villous tree development.

Although in vivo trophoblast fusion is extremely efficient and produces a complete syncytial sheath over the villous tree, fusion induced through established biochemical factors can at best produce partial syncytial patches in cultured trophoblasts

Received: November 4, 2019
Accepted: November 27, 2019
Published: November 27, 2019

DOI: 10.1021/acsami.9b19906
ACS Appl. Mater. Interfaces 2019, 11, 47810−47821

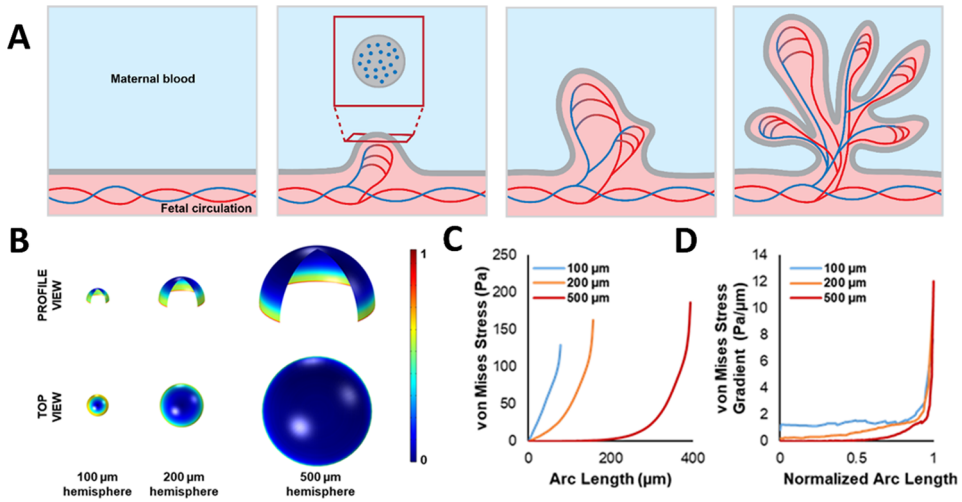

Figure 1. Endogenous tissue stress patterns arise during villous tree developmental morphogenesis. (A) Schematic of the budding morphogenesis process by which the placental villous tree arises during tissue development. The villous tree is coated with a fully fused syncytiotrophoblast (STB) layer that is challenging to perfectly recreate in vitro through either chemical or genetic means. Inset shows the top view of the multinucleated STB at the villous tree tips. (B–D) Finite element models to estimate the endogenous stress patterns that arise due to cell-generated tension in the cell sheet at bud sites during villous tree development. (B, C) von Mises stress profiles in idealized buds of 100, 200, and supraphysiologically large 500 μm diameters demonstrate increased endogenous stress at the bud edges, which reduces toward the bud apex (color scale bar normalized across the stress range observed). (D) Elevated stress gradients are expected across the surface of the bud, only in sufficiently small buds that match expected physiological dimensions.

with low efficiency.[4,12,13] Our present inability to consistently control fusion in in vitro models of the STB hampers efforts to engineer placental model culture systems as defects in fusion will dominate in studies of transport between maternal and fetal body compartments.[14] The mixture of fused and unfused cells may also play a role in dictating active and passive transport profiles across the STB layer.[15] Hence, alternative approaches to predictively and robustly drive fusion in trophoblast cells would have a considerable and fundamental impact on our ability to develop culture models and ultimately therapies for pregnancy-related diseases.

To investigate alternative and potentially synergistic strategies for syncytial formation, we considered whether the biomechanical stress profiles that arise during development of the villous tree structure might themselves play a role in trophoblast fusion. The villous tree grows from a placental bud in a process of repeated budding morphogenesis to produce the final villous architecture (Figure 1A). Three-dimensional tissue structures can generate complex mechanical stress profiles that arise from endogenous cell-generated tension[16−18] and these patterns are known to affect differentiation,[19] embryogenesis,[20] tissue homeostasis,[21] and disease progression.[16] However, whether mechanical forces play a role in driving trophoblast fusion remains unknown. If true, establishing a technique to recreate the mechanical features present during developmental formation of the STB during villous tree growth would be of considerable value in engineering advanced placental tissue discovery models for drug screening and therapeutic development.

Since tissue stresses can be modulated by manipulating the shape of microscale cultures, we leverage 2D micropatterning techniques to recreate the biomechanical stress patterns present during the budding morphogenesis process of placental villous tree development and investigate whether these stress patterns could enhance fusion efficiency in vitro. We test this idea in both standard cell lines used for studies of trophoblast fusion (BeWo choriocarcinoma cells) and in primary villous cytotrophoblasts (vCTB) cells isolated from human placentas at delivery. Our findings demonstrate that fusion can be synergistically enhanced and spatially directed using the biomimetic culture geometries. Furthermore, we demonstrate that these patterns direct spatial production of pregnancy hormones. These studies demonstrate that villous trophoblast fusion is mechanically sensitive and can be directly regulated by endogenous stress, indicating that manipulating biophysical cues is a viable and novel strategy to improve fusion in in vitro culture models. More importantly, these studies demonstrate that recreating mechanical cues present during morphogenesis could lead to improved placental tissue engineering approaches. Such strategies could ultimately lead to improved benchtop discovery and drug screening assays and, more broadly, contribute toward our understanding of mechanoregulatory processes in pregnancy disorders.

MATERIALS AND METHODS

Unless otherwise stated, all cell culture materials and supplies were purchased from Thermo Fisher Scientific (Ottawa, ON), and chemicals were purchased from Sigma-Aldrich (Oakville, ON).

Finite Element Models of Micropatterned Contractile Cell Monolayer. Finite element analysis was conducted to estimate the approximate stress patterns present in the buds of placental trees and in the confined culture models developed here to simulate those culture conditions. Simulations were conducted using COMSOL Multiphysics 5.3a (COMSOL, Inc., Burlington, MA) to capture the contractile effect of a cluster of cells anchored to a fixed underlying geometry. The simulation method was adapted from previous reports[17] and made use of a temperature-based contractile element to simulate contractile behavior. Briefly, the desired circular geometry was modeled as a 2D axisymmetric system with two layers: a 20 μm-thick active top layer representing the cells (isotropic elastic modulus: 500 Pa; Poisson's ratio: 0.499; thermal conductivity: 10 W × M^{-1} × K^{-1}; coefficient of expansion: 0.05 K^{-1}) and a 4 μm-thick passive layer representing the underlying substrate (isotropic elastic modulus: 100 Pa; Poisson's ratio: 0.499), with a fixed displacement boundary condition applied to the bottom surface. A 3D, bud-like geometry was created by adapting our 2D model to create a hemispherical, dome-

DOI: 10.1021/acsami.9b19906
ACS Appl. Mater. Interfaces 2019, 11, 47810−47821

like structure with a zero-displacement condition on the bottom of the passive surface. A 5 K temperature drop was applied to create an isotropic monolayer contraction in the active layer. The von Mises stress and von Mises spatial stress gradients at the bottom of the passive surface were recorded and reported for circular patterns with diameters of 100, 200, and 500 μm. A large simulated circular sheet of 5000 μm diameter was used to approximate the equivalent stress patterns in the 2D unconfined condition. The magnitudes of monolayer contraction were varied by adjusting the temperature drop applied to the material.

Microfabrication of Confined Culture Substrates. Agarose microwells with adhesive substrates were fabricated as previously described.[22] SU-8 molds with desired microfeatures (circular micropattern with various diameters) were first fabricated by photolithography using standard techniques.[23] Briefly, a 15 μm-thick SU-8 photoresist (MicroChem, MA) layer was spin-coated onto a clean 50 mm × 75 mm glass slide, subsequently soft-baked at 70 °C for 2 min and then hard-baked at 100 °C for 5 min. The SU-8 coated glass slide was then covered with a mask (CAD/ART Services) containing designed circular patterns and exposed to UV light for 30 s to polymerize the resist. The slide was then immersed in SU-8 developer with gentle agitation, where an unpolymerized SU-8 monomer is washed away. The resultant mold with microfeatures was then postbaked at 100 °C for 5 min. The mold was treated with the silanization agent (tridecafluoro-1,1,2,2-tetra-hydrooctyl)-1-trichlorosilane (United Chemical Technologies, Bristol, PA) under vacuum conditions overnight to facilitate the mold release of the patterned PDMS layers. PDMS (Sylgard 184, Dow Corning) stamps with pillars structures were then fabricated using soft lithography by casting mixtures of 1:10 (w/w, curing agent to base) PDMS prepolymer on top of the SU-8 mold and curing in an oven at 70 °C for 1 h. The PDMS stamps were placed feature-side down on a 12 mm glass coverslip and plasma-oxidized to increase hydrophilicity of the PDMS surface to allow better wicking of the cell-repellent aqueous molten agarose solution. A 10 μL droplet containing a mixture of 1% agarose solution and ethanol (v/v, 3:2) was melted on a hot plate, pipetted onto the sides of the stamps, and then perfused through the pillars. The coverslips were placed under vacuum in a desiccator overnight to allow gelation and dehydration. The PDMS stamps were peeled off vertically using tweezers. Prior to cell seeding, the microwells were sterilized under UV light for 45 min and incubated with 25 mg/mL fibronectin solution for 1 h at room temperature.

Cell Culture and Isolation. BeWo cells (CCL-98 clone), from American Type Culture Collection (ATCC; Rockville, MD), were cultured in Dulbecco's modified eagle medium (DMEM)/F-12 with phenol red and supplemented with 10% fetal bovine serum (FBS; Hyclone, Tempe, AZ) and 1% penicillin−streptomycin (Hyclone). BeWo cells with passage number lower than 20 were used at a density of 2×10^5 cells/mL. Twenty-four hours after seeding cells on agarose gels with the described microwells, cells were treated with 20 μM forskolin (Sigma-Aldrich, F6886) for 48 h. The forskolin-containing medium was changed daily during the experiments. Human primary vCTBs, were obtained from term placentas arising from the vaginal delivery of uncomplicated pregnancies after the ethical approval from the CHUM St-Luc Hospital (Montreal, QC, Canada) and informed patient consent. vCTB cells were isolated based on the trypsin-DNase/Percoll method.[24] Briefly, placental tissue was exposed to consecutive digestions with trypsin and DNAse. The supernatant of each bath was collected, pooled, and then separated within a Percoll gradient. Mononuclear villous trophoblasts were immunopurified using an autoMACS (Miltenyi Biotec, Santa Barbara, CA). All vCTB preparations used in this study were at least of 95% purity after cell sorting.[25,26] Under sterile conditions, purified vCTB was mixed in a 1:10 solution of FBS and sterile dimethyl sulfoxide (DMSO) and mixed gently by flipping. Cells were frozen overnight at −80 °C and transferred to a liquid nitrogen tank until usage. Primary vCTBs were seeded at a density of 1.6×10^6 cells/mL. These cells do not replicate in vitro and spontaneously differentiate into multinucleated STB over 72 h of culture.[9,25] vCTBs were cultured in high-glucose DMEM, supplemented with 10% FBS and 1% penicillin−streptomycin.

Traction Force Microscopy Substrate Preparation. To conduct traction force microscopy (TFM) experiments, polyacrylamide hydrogels with known mechanical properties containing fiducial markers were patterned with fibronectin circular patterns, using a modified microcontact printing protocol adapted from Rape et al.[27] Briefly, PDMS molds were prepared as previously described, with stamps cut to 10 mm × 10 mm squares, soaked in 70% ethanol for 10 min, and thoroughly dried under a dry nitrogen stream. Activated fibronectin was prepared by adding 3.6 mg/mL sodium metaperiodate to a 0.1 mg/mL fibronectin mixture and incubated at room temperature for 30 min. PDMS stamps were inked with 20 μL of activated fibronectin and incubated at room temperature for 45−60 min after which the stamps were washed with water and dried. To provide a release surface for the polyacrylamide gels, 18 mm coverslips were buffed with RainX (commercially available) and then subjected to a short 30 s of plasma treatment (PlasmaEtch; 200 mTorr pressure, 20 ccm flow rate, and 60 W RF power) to facilitate release. Inked PDMS stamps were gently placed face down on the release coverslips for 10 min to transfer the circular fibronectin patterns to the release surface. A solution of 100 μL 40% acrylamide, 150 μL 2% bis-acrylamide, 645 μL PBS, 1.5 μL tetramethylethylenediamine, and 100 μL of 1% ammonium persulfate (Bio-Rad) was prepared with 0.5% volume of 0.5 μm diameter carboxylate-modified fluorescent beads (FluoSpheres, Invitrogen). Immediately after mixing, 50 μL of this solution was pipetted onto a coverslip that had previously been silanized by immersion in 0.4% 3-(trimethoxysilyl)propyl methacrylate in acetone. The patterned coverslip was then placed face down on the droplet, which was allowed to polymerize. After 15 minutes, the top coverslip was removed, and the patterned gels were washed three times in PBS, sterilized under a UV germicidal lamp for 45 min, and stored at 4 °C until use. These gel formulations have previously been characterized by shear rheometry (G = 1.3 kPa).[28]

Traction Force Microscopy. TFM substrates were incubated in complete DMEM for 2 h at 37 °C and seeded with BeWo cells, which were allowed to attach and spread overnight. Individual coverslip-mounted TFM gels were gently rinsed with PBS and transferred to a magnetic 18 mm coverslip chamber (Chamlide CMB, Quorum Technologies; Puslinch, ON, CA). Supplemented DMEM (1 mL) was added to the chamber for the duration of the experiment. The chamber was then placed into a circular 35 mm microscope stage top insert (ibidi GmbH; Gräfelfing, Germany). To capture both the stressed and relaxed gel conditions required for the traction force analysis, red fluorescent images of the uppermost layer of embedded beads were first captured along with phase-contrast images of the selected colonies using a spinning disc confocal microscope (20× objective, IX-73, Olympus). Cells were then killed with 1% (w/v) sodium dodecyl sulfate (SDS) and the beads were imaged to obtain the zero-stress state at each TFM position.

To analyze the TFM image sets, template alignment, particle image velocimetry (PIV), and Fourier transform traction cytometry (FTTC) ImageJ plugins were used for the TFM analysis, following previous protocols.[29] Briefly, both stress and relaxed fluorescent bead images were combined into a stack and aligned to account for experimental drift. The bead displacements were estimated by PIV following an iterative procedure. With each iteration, the interrogation window was made smaller to produce an ultimate displacement field grid with dimensions of 6.75 μm by 6.75 μm with an average of five beads per interrogation window. A dynamic mean test for low correlation values was performed on the resulting displacement field images to remove erroneous vectors and replace them with an average displacement value obtained from the neighboring final interrogation windows. Traction force fields could then be reconstructed with the FTTC plugin. Displacement and the corresponding stress values were extracted from the vector field images along various lines passing through the center of the colony and plotted as line graphs.

Human Chorionic Gonadotropin Secretion Analysis. Conditioned cell culture media samples were collected after 48 h of forskolin induction from single wells in a 12-well plate in which arrays of micropatterned islands were cultured. Supernatants were

DOI: 10.1021/acsami.9b19906
ACS Appl. Mater. Interfaces 2019, 11, 47810−47821

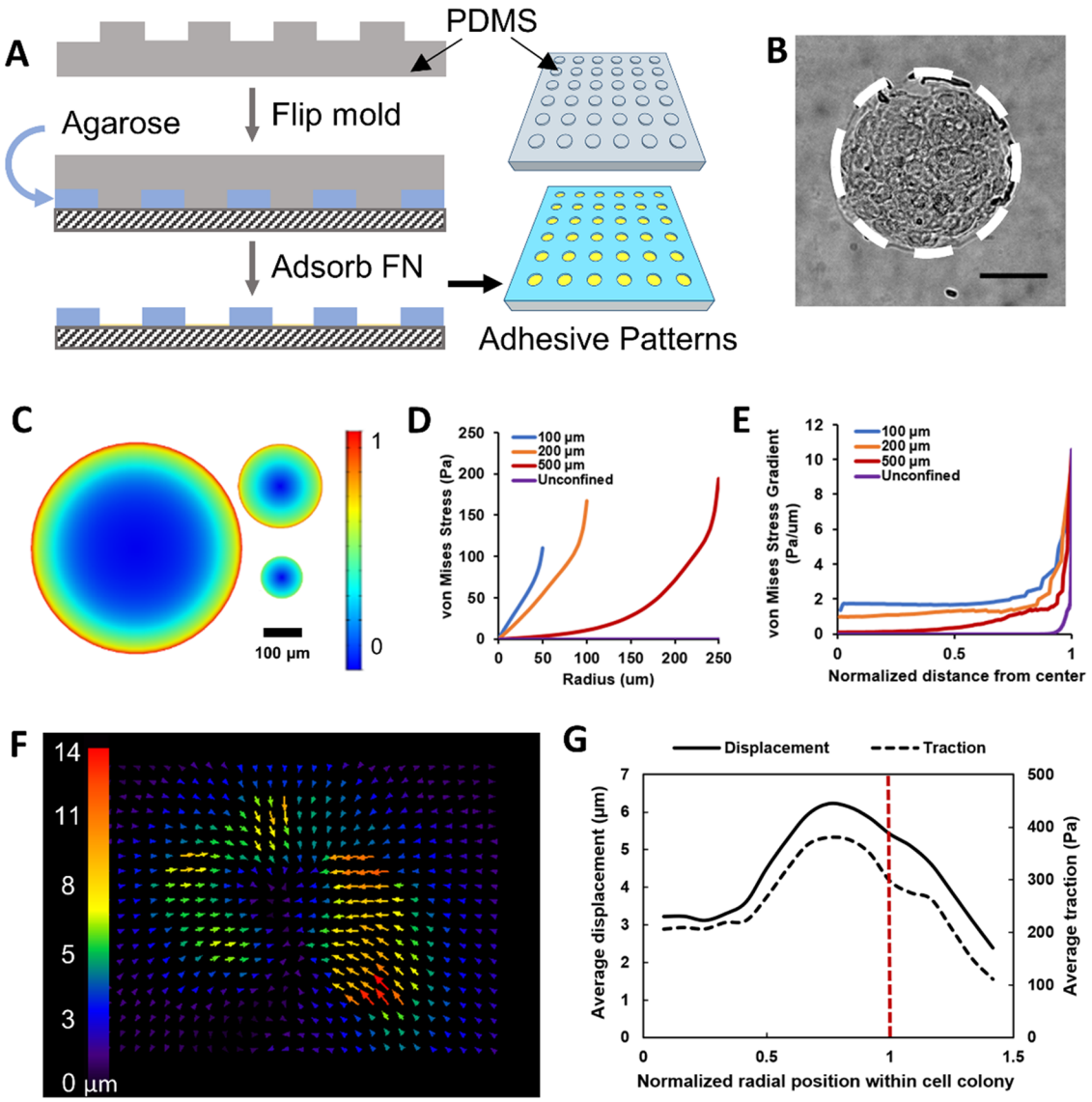

Figure 2. Micropatterned two-dimensional cell culture substrates recreate endogenous stress gradient patterns expected from three-dimensional budding structures. (A) Fabrication process for micropatterned cultures. (B) Representative bright field image of BeWo cells in confined micropatterned islands. (Scale bar = 100 μm). (C–E) Finite element models demonstrating expected endogenous stress patterns arising from cell contractility in micropatterned culture. (C) Heat map of predicted relative von Mises stress in 500, 200, and 100 μm diameter patterns (color scale bar normalized to the highest stress value). (D) Calculated stress magnitude and (E) radial stress gradient for the micropatterned culture diameters used in this work. (F, G) Traction force microscopy experiments demonstrate that (F) displacement fields follow expected radial inward orientation and (G) average radial displacement (solid line; left axis) and traction stresses (dashed line; right axis) for forces generated across a representative 100 μm colony of cells match the expected stress patterns arising from endogenous contractility, with peak stresses observed at the colony edge. Spatial data normalized to colony size (red dashed line indicating colony edge; experiment repeated three times with similar results).

centrifuged and stored at −20 °C prior to the assay. Secretion of beta human chorionic gonadotropin (β-hCG) in the collected media was evaluated by enzyme-linked immunosorbent assay (ELISA;EIA-1911; IBL International, Toronto, ON, Canada), following the manufacturer's recommended protocols. Aliquots of the collected media were incubated in enzyme conjugate-coated microtiter wells for 15 min at room temperature. The absorbance of each well at 450 nm was determined with a microtiter plate reader. β-hCG secretion levels were normalized against the total number of cells in each sample, as assessed via fluorescent imaging and semiautomated counting (ImageJ; NIH).

Immunostaining. Cells were fixed in 4% (w/v) paraformaldehyde (Sigma-Aldrich, St. Louis, MO) in phosphate-buffered saline (PBS) solution for 15 min at room temperature. We found that syncytial patches (fused trophoblasts) were very weakly adhered to the underlying substrates, and to prevent cell detachment during the extensive washing steps, a thin layer of porous polyacrylamide hydrogel was polymerized over the tissues after fixation. The prepolymer (containing 7.5% (v/v) acrylamide (40% w/v, Bio-Rad Laboratories, Hercules, CA), 2.45% (v/v) cross-linker *N*,*N*-methylene-bis-acrylamide (BIS, 2% w/v, Bio-Rad Laboratories, Hercules, CA), 0.1% (w/v) ammonium persulfate (Bio-Rad Laboratories, Hercules, CA), and 0.15% (v/v) catalyst *N*-*N*-*N*-*N*-tetramethylethylenediamine (Sigma-Aldrich)) was cast over the fixed cells and allowed to polymerize under a glass coverslip. This process was confirmed to have no effect on the immunostaining results (data not shown). Samples were washed twice with PBS and permeabilized in 0.1% (v/v) Triton X-100 (Sigma-Aldrich) in PBS solution for 15 min and washed twice with PBS again. Samples were incubated in 2.5% (v/v) goat serum (Sigma) in PBS for 2 h at room temperature to prevent nonspecific binding. For indirect staining, cells were first incubated overnight with anti-E-cadherin antibody (1:200, Abcam,

DOI: 10.1021/acsami.9b19906
ACS Appl. Mater. Interfaces 2019, 11, 47810–47821

ab1416) or anti-hCG antibody (1:500, Thermo Fisher, #14-6508-82) in goat serum solution. For secondary staining, cells were washed twice with PBS and then incubated with goat anti-mouse IgG H&L (Alexa Fluor 488) antibody (1:1000, Abcam, ab150113) in blocking agents for 3 h. For direct staining, cells were incubated with 1:200 DAPI (Invitrogen) and FITC-phalloidin (Invitrogen) in goat serum solution for 2 h at room temperature. Samples were then washed thoroughly with PBS before imaging.

Image Collection and Processing. Fusion ratios of BeWo cells after 48 hour forskolin treatment and vCTBs after 72 hour primary culture were determined by image analysis based on immunofluorescent localization of E-cadherin and DAPI-labeled nuclei. Imaging was performed on an inverted fluorescent Olympus microscope (Olympus, IX73) outfitted with a CMOS Flash 4.0 camera and MetaMorph software (version 7.8.13.0). Subsequently, the E-cadherin, β-hCG, and DAPI images were recolored, merged, and analyzed using ImageJ (NIH).

Analysis of Cell Fusion. For BeWo cells, any cluster of three or more nuclei enclosed within an E-cadherin boundary was considered a syncytium, as per established characterization guidelines.[30] The total number of nuclei (T), syncytium number (S), and total nuclei number in fused syncytium (F) were counted. The ratio of cell fusion was calculated using the following standard equation: $(F - S + 1)/T \times 100$. Characterization of fusion in vCTBs is typically more challenging than in BeWo cells as cells do not spread well to show well-defined E-cadherin-labeled membranes. Hence, fusion ratios were calculated by dividing the number of E-cad expressing cells over the total number of cells cultured on micropatterned adhesive islands, consistent with standard protocols.[31]

Statistical Analysis. Comparative data analysis of fusion ratio of BeWo cells and vCTBs was based on results obtained from three independent experiments conducted on different days. The fusion ratios of all filled wells were averaged, and standard deviations were calculated based on three repeated independent experiments. Statistical significance of fusion ratios among different micropattern culture dimensions was analyzed using a two-tailed, one-way ANOVA with a Holm−Sidak posthoc pairwise comparison test. All statistical analyses were conducted in SigmaStat 3.5 (Systat Software Inc., San Jose, CA).

RESULTS

Estimates of Stress Patterns during Villous Tree Budding Morphogenesis. To evaluate the endogenous stress patterns that arise during villous tree growth, three-dimensional (3D) finite element simulations were conducted. 3D biological structures have been shown to balance tensile forces on the surface and compressive stresses within the tissue,[18] and hence, a characteristic endogenous stress profile would be expected across a budding structure. To approximate stresses in both the villous tree tips and in micropatterned adhesive islands, we simulated a uniform volumetric contraction of the cells against a rigid underlying hemispherical substrate. The geometry of the bud diameters was estimated to vary between 50 and 200 μm, based on reported characteristics of the villous tree developmental stages.[32] We hence developed models of physiological (<200 μm diameter) and supraphysiological (500 μm diameter). Although the absolute values for stresses reported are dependent on multiple assumptions that are specific to certain cell type and culture conditions, the characteristic stress profiles observed should be reasonably accurate.

The reported von Mises stress values express the distortion energy density at a particular point in the contractile hemispherical cell monolayers (Figure 1B−D). In all geometries, areas of high stress are predicted at the peripheries, while lower stresses were reported in the center (Figure 1C). In physiologically-realistic structures smaller than 200 μm in diameter, appreciable stress levels were noted across the cell surface, while supraphysiologically large structures exhibited large central areas with negligible stress levels. To better capture this difference, we present the data as stress gradients normalized to position across the arc surface (Figure 1D), which demonstrates that elevated stress gradients exist throughout the central region of the buds only for smaller physiological bud sizes. Hence, patterns of endogenous cellular stress can arise during the dynamic process of villous tree morphogenesis.

Micropatterned 2D Cultures Are Expected To Generate Similar Endogenous Stress Profiles. Micropatterned adhesive islands were fabricated successfully on glass substrates using the described agarose perfusion procedure (Figure 2A), with diameters ranging from 50 to 500 μm. Bright field microscopy demonstrates high uniformity and success rates in pattern fabrication (data not shown). To confirm that cells can be cultured in the micropatterned wells, BeWo choriocarcinoma cells were seeded on the surfaces. Cells adhered only to the adhesive surfaces where they formed well-defined circular micropatterned islands (Figure 2B).

To predict stresses in the micropatterned adhesive islands, we simulated tension-generating cells on circular resistive substrates of various diameters to determine the endogenous stress profiles arising from culture in these geometries (Figure 2C−E). In unconfined cultures, stresses remained uniformly low. Similar to the 3D simulations, for cells cultured in circular micropatterns, stress varied from zero at the center to a maximal stress at the edge (Figure 2C,D). Although the maximum and minimum von Mises stresses were roughly similar across all micropatterned culture diameters, the distribution of stress within the pattern varied considerably. Stresses in the 100 and 200 μm diameter patterns increased rapidly from the center to the edge of the culture. Stresses in the 500 μm diameter patterns were relatively low and uniform in the central area of the culture but increased sharply toward the culture edges (Figure 1C). This suggests that for this specific application, the large central areas of the 500 μm diameter culture experience mechanical culture conditions closer to that of the unconfined culture condition, and that "edge" effects play a significant role in the pattern only when the pattern is sufficiently small.

To better describe the variations in stress across the micropatterned surfaces, we calculated the stress gradients and normalized them to the pattern diameters (Figure 2E). No stress gradients were observed in the unconfined culture, and as is the case with the 3D bud simulations, increased stress gradients are observed across the culture surface with decreasing micropattern size. Stress gradients were generally appreciable and more for micropatterned culture islands that were 200 μm in diameter or smaller (Figure 1D).

These simulations present very similar profiles to the stress patterns expected during 3D budding morphogenesis and demonstrate that micropatterned 2D surfaces may adequately recreate the endogenous stress profiles expected within cells during the budding morphogenesis process. It is hence reasonable to recreate the endogenous tension biomechanics of the 3D placental tree budding structures in 2D micropatterned cultures, similar to other studies that leverage micropatterning to understand developmental mechanobiology.[17,19]

Experimental Verification of Trophoblast Stress Patterns in Micropatterned Cultures. To verify that

DOI: 10.1021/acsami.9b19906
ACS Appl. Mater. Interfaces 2019, 11, 47810−47821

trophoblast cells generate similar patterns of traction forces in micropatterned cultures as other adherent cells,[33] we conducted traction force microscopy experiments on micropatterned cultures of BeWo cells. As expected, cells in small circular colonies generated patterns of bead displacements toward the colony center, indicating contractile force generation (Figure 2F). Bead displacements were radially averaged and used to calculate traction stresses across the sample (Figure 2G). These stresses match the stress gradient patterns expected within the micropatterned colony, based on finite element simulations (Figure 2C,D).

Although the models do predict sharp stress peaks at the micropattern edge, the traction force microscopy measurements demonstrate significant stresses that extend beyond the micropattern and into the surrounding hydrogel. This is an expected artifact as deformable substrates surrounding the contractile pocket of cells distribute stresses beyond the colony itself. The micropatterned adhesive surfaces do not deform, and hence, stress is concentrated at the colony boundaries and redirected within the culture. Furthermore, the need for soft and deformable substrates to conduct such experiments may significantly alter the contractile stresses generated by cells themselves,[27] compared to the culture on micropatterned glass. Hence, the absolute stress magnitudes determined through any traction-based technique cannot be directly compared to endogenous stresses generated on rigid glass substrates. The stress patterns, however, should remain generally consistent. To confirm this, we conducted finite element simulations (Figure S1) to verify that stress patterns across a micropatterned island remain similar, even for differences in cell-generated contractile strain.

Taken together, these results confirm that stress patterns expected through finite element modeling are recreated by trophoblasts cultured in micropatterned islands.

Micropatterned Cultures Support Trophoblast Fusion. To confirm that cultured cells can be induced to fuse in the micropatterns, seeded BeWo cells were maintained in basal media (Figure 3A) or induced with 20 μM forskolin (Figure 3B) for 48 h, which is well established to induce fusion in this cell type in standard culture.

Fusion is commonly assessed by evaluating the patterns of E-cadherin expression, where disruption of the E-cadherin boundary around individual cells is regarded as the hallmark of trophoblast fusion.[34] When cultured on the micropatterned surfaces in basal media, cells adhered only to the adhesive surfaces, where they formed well-defined micropatterned islands. Strong E-cadherin expression was observed around all individual cells, and no spontaneous fusion events were observed in any of the control experiments (Figure 3A). Filamentous actin (f-actin) structures formed readily throughout the cultures, as expected for cells in mechanically stressed conditions. Hence, endogenous mechanical tension induced by circular micropatterns alone is not sufficient to induce fusion in this cell line.

After induction with forskolin for 48 h, E-cadherin could not be detected between cytotrophoblasts in the center of the micropatterns, indicating successful fusion and syncytium formation. This is supported by the extensive rearrangement of f-actin cytoskeleton accompanying cell fusion, where the once prominent stress fibers were disrupted into small circular foci. These results are consistent with previous reports that have established these biomarkers as signature characteristics of cell fusion[34,35] and confirm that BeWo cells retain their capacity for fusion and expression of standard characteristic markers of fusion in the present micropatterned culture system.

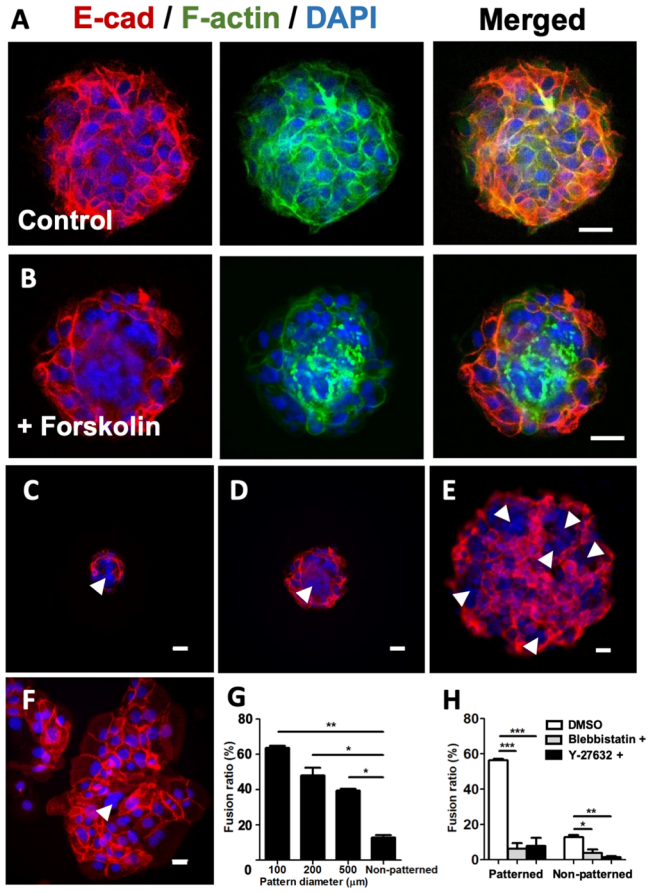

Figure 3. Fusion efficiency is synergistically enhanced and spatially directed in sufficiently small micropatterned colonies after 48 h forskolin induction. (A, B) BeWo cells are successfully cultured on 200 μm diameter patterns in (A) basal media and (B) fusion induction media (forskolin, 20 μM). Fusion is accompanied by distinct morphological changes in f-actin (green) and disappearance of E-cadherin (red) from around cell nuclei (blue) within the micropatterned well (scale bars = 50 μm). (C–F) Representative images of fusion-induced BeWo cells in micropatterned islands with diameters of (C) 100 μm, (D) 200 μm, (E) 500 μm, and (F) on nonpatterned substrates (scale bars = 50 μm). Arrows indicate observed syncytial patches with characteristic disappearance of E-cadherin (red) around the nuclei (blue). (G) Fusion ratio was greatly enhanced under micropatterned culture compared to nonpatterned conditions (data reported as mean ± standard deviation, $n = 3$; $^{*}p < 0.05$, $^{**}p < 0.01$ by two-tailed, one-way ANOVA with Holm–Sidak posthoc comparisons). For clarity, not all significant differences are shown, but every experimental condition was significantly different compared to every other experimental conditions. (H) Inhibition of mechanosensing myosin II with 50 μM Blebbistatin and ROCK with 10 μM Y-27632 reduced fusion ratios to <10% in both 100 μm culture patterns and in nonpatterned culture conditions ($n = 3$–9; data reported as mean ± standard deviation; $^{*}p < 0.05$, $^{**}p < 0.01$, or $^{***}p < 0.001$ by two-tailed, one-way ANOVA with Holm–Sidak posthoc comparisons).

BeWo Cell Fusion Is Enhanced on Micropatterned Adhesive Substrates. To investigate the effects of tissue dimensions and geometric confinement on BeWo cell fusion, micropatterned circular adhesive islands with diameters of 100, 200, and 500 μm (Figure 3C–E) and unconfined controls

DOI: 10.1021/acsami.9b19906
ACS Appl. Mater. Interfaces 2019, 11, 47810–47821

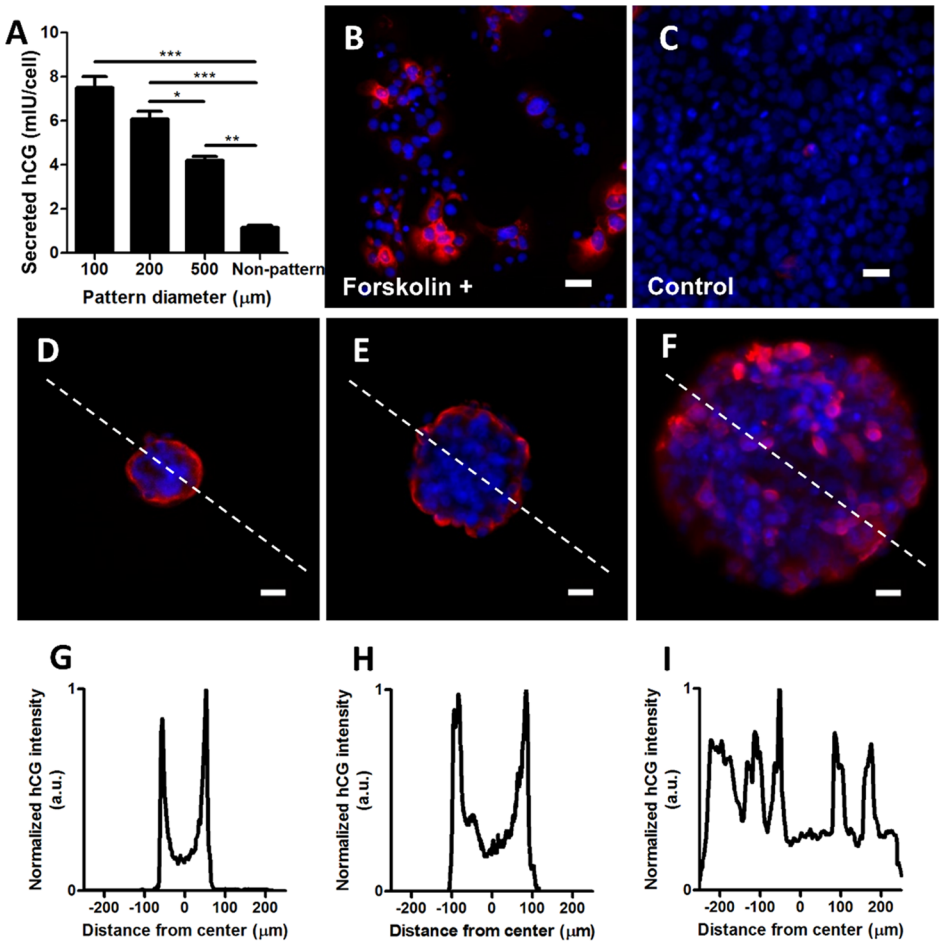

Figure 4. Characterization of secreted and intracellular β-hCG expression from BeWo cells in nonpatterned and micropatterned cultures. (A) Secreted β-HCG in the culture media normalized to the number of cells is significantly enhanced in smaller micropatterned culture conditions (data reported as mean +/− standard deviation, $n = 3-7$; $^{*}p < 0.05$, $^{**}p < 0.01$, $^{***}p < 0.001$ by two-tailed one-way ANOVA with Holm−Sidak posthoc comparisons). (B, C) β-hCG expression is induced in nonpatterned culture within 48 h of (B) forskolin treatment compared to (C) control culture conditions. (D−F) Representative images showing spatial distribution of intracellular β-HCG within micropatterns of diameters (D) 100 μm, (E) 200 μm, and (F) 500 μm after forskolin induction. (G−I) Normalized β-HCG fluorescent intensity along the indicated white dashed lines. Similar trends were observed on microtissues analyzed across three independent experiments. (red = intracellular β-hCG; blue = nuclei; scale bars = 50 μm).

(Figure 3F) were prepared and used as culture substrates during forskolin-induced fusion. In unconfined cultures, BeWo cells spontaneously formed uncontrolled patches of varying sizes. The fusion ratio across these standard unconfined cultures, at this level of forskolin concentration and induction time, was ∼15%. In contrast, fusion efficiency on the micropatterned surfaces was significantly higher and ranged from 40 to over 60%, with the smallest micropattern surfaces producing the highest fusion ratios (Figure 3G). Fused syncytial patches formed in the central regions of the 100 and 200 μm diameter microwells and formed sporadically in the larger microwells (white arrow heads in Figure 3A−C). Interestingly, the size of these syncytial patches was roughly similar across all the islands. These results demonstrate that biochemically induced fusion can be both synergistically enhanced and spatially directed via culture in micropatterned adhesive islands. To confirm that these findings are mediated by mechanical tension, we conducted mechanosensing inhibition experiments to target myosin II activity in the cytoskeleton (via treatment with 50 μM Blebbistatin) and the ROCK signaling pathway (via treatment with 10 μM Y-27632 inhibitor). In both cases, fusion ratios were significantly reduced to less than 10% in both 100 μm diameter culture patterns and in unconfined control experiments (Figure 3H, Figure S2). These results confirm that the observed increases in fusion are driven by mechanobiological activity arising from culture in the micropatterned islands.

Secreted and Intracellular β-hCG Expression Patterns in Circular BeWo Microtissues. β-human chorionic gonadotropin (β-hCG) is essential for fetal growth and development, and synthesis and secretion of β-hCG are considered a classical biochemical marker of trophoblast fusion,[36,37] but excessive production of β-hCG is also associated with placental dysfunction.[38−40] The factors that distinguish regular versus excessive production of β-hCG in fused BeWo cells remain unknown.

We first conducted standard assays for β-hCG expression by analyzing the levels of secreted β-hCG in the culture medium via ELISA for forskolin-induced fusion in unconfined culture and for culture in micropatterns. As expected, on a per cell basis, secreted β-hCG levels significantly increased with decreasing micropattern size, with over a 4-fold increases in secretion in 100 μm diameter cultures compared to non-patterned conditions (Figure 4A). These results are consistent

DOI: 10.1021/acsami.9b19906
ACS Appl. Mater. Interfaces 2019, 11, 47810−47821

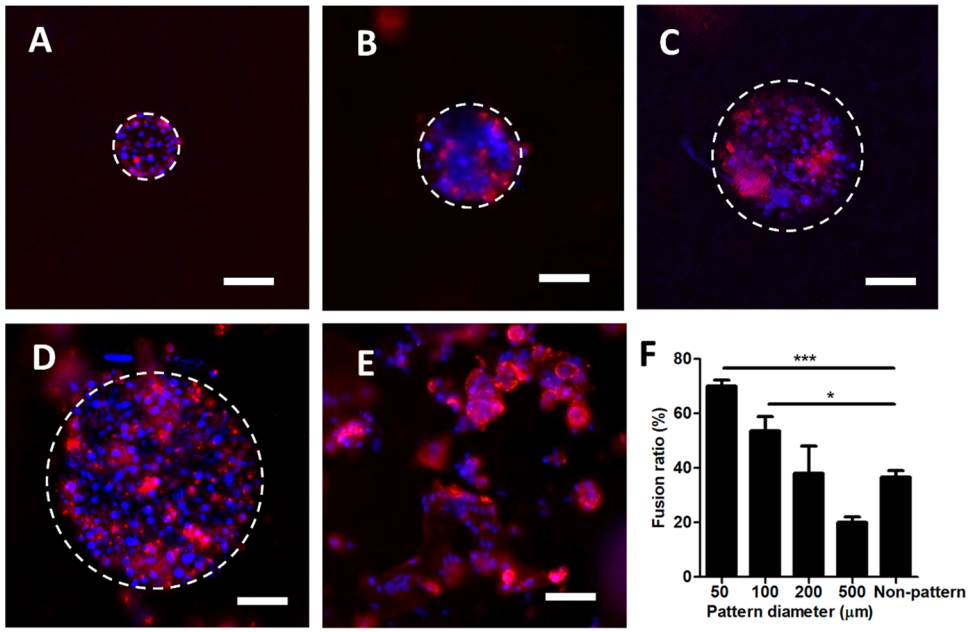

Figure 5. Increased spontaneous fusion of primary vCTBs under micropatterned culture. (A–E) Representative figures of spontaneous fusion of micropatterned vCTBs cultured on adhesive islands with diameters of (A) 50 μm, (B) 100 μm, (C) 200 μm, and (D) 500 μm and (E) on nonpatterned substrates. Cultures labeled with E-cadherin (red) and DAPI (blue) to evaluate fusion efficiency. (Scale bars = 50 μm). (F) Fusion ratios were greatly enhanced in the micropatterned culture with the smallest dimensions comparing to nonpatterned culture conditions. (data reported as mean ± standard deviation for $n = 3$ independent experiments; $^{*}p < 0.05$ or $^{***}p < 0.001$ by two-tailed, one-way ANOVA with Holm–Sidak posthoc comparisons).

with our observations of increased levels of fusion in micropatterned cultures and validate functional production of pregnancy-related hormones through fusion in micropatterned cultures.

However, measurements of secreted protein do not provide any insight into spatial production of the protein, and the predictable fusion patterns afforded by this micropatterned culture system provide an excellent model system with which to analyze spatial production of these factors. We hence examined intracellular patterns of β-hCG via immunofluorescence after forskolin-induced fusion. We first verified that in our hands, forskolin is required for intracellular β-hCG production (Figure 4B,C) and observed brightly stained heterogeneous patches in the unconfined culture, consistent with previous literature reports.[41] Untreated cells showed minimal signs of intracellular β-hCG expression. In contrast, intracellular β-hCG on the micropatterned substrates was strongly expressed at the microtissue edges for small (<200 μm diameter) patterns (Figure 4D,E) but was randomly distributed in larger cultures (Figure 4F). Line intensity plots across representative microtissue colonies demonstrate clean patterns of β-hCG localized to the syncytia edges and relatively low expression of β-hCG within the fused syncytial patch (Figure 4G,H). In contrast, β-hCG expression was generally greater on larger diameter patterns (500 μm; Figure 4F,I), with sporadic high expression throughout the culture and generally higher levels observed in the background (Figure 4I).

We verified via costaining that fusion and intracellular β-hCG expression occur simultaneously in small patterns (Figure S3). The observed expression levels and hCG production patterns correspond to the expected E-cadherin boundaries that surround small patterned cultures and are within both large patterns and unconfined cultures. Although the mechanism by which intracellular β-hCG is secreted into the media is not clear, it is reasonable to conclude that intracellular proteins are being secreted where they are being produced, at the boundaries between fused syncytial patches. This prompts us to speculate that a perfectly fused syncytium with no boundaries would ultimately secrete lower hCG levels than imperfectly fused syncytia, which would be consistent with known upregulation of hCG in conditions of placental dysfunction. However, in standard cultures, these observations are confounded by an inability to independently specify the fused area from the defect edge, suggesting further applications for micropatterned surfaces as a platform technology with which to study functional results of improperly fused tissues.

Human Primary vCTB Fusion Is Increased on Micropatterned Adhesive Substrates. The BeWo cell type used in these experiments is broadly accepted as a model for fusion of human placental trophoblasts due to a well-established capacity to fuse into an STB with expected changes in other biomolecular parameters. To further confirm that the high-efficiency fusion levels observed in micropatterned substrates are not an artifact of using the choriocarcinoma-derived BeWo cell line, we conducted additional experiments with primary human vCTBs. Culture of these primary cells is significantly more challenging than that of BeWo cells as they are from a limited supply of cells, do not proliferate in vitro, and have variable adhesion characteristics. Additionally, they are considerably smaller than BeWo cells as vCTBs typically spread on culture surfaces to areas of $\sim 1-2 \times 10^{-3}$ mm^2/cell, compared to BeWo cells, which spread to areas of $\sim 3-4 \times 10^{-3}$ mm^2/cell. Hence, smaller micropattern dimensions (50 μm diameter) were included to accommodate the smaller cell size and their inability to proliferate and fill the well.

Primary isolates from term placenta were seeded on circular adhesive islands with diameters of 50, 100, 200, and 500 μm (Figure 5A–D), along with unconfined conditions as control

DOI: 10.1021/acsami.9b19906
ACS Appl. Mater. Interfaces 2019, 11, 47810–47821

(Figure 5E). Significantly increased fusion ratios were achieved in microtissues with diameters of 100 μm and smaller compared to unconfined controls. For microtissues of 50 μm diameter, an average of 70% fusion ratio was achieved, compared to less than 40% in unconfined culture (Figure 5F). No significant differences were found in fusion ratios for patterns of 200 μm diameter or greater, although this might be due to the reduced size of primary vCTB cells and their inability to proliferate in vitro, compared to BeWo cells, which makes it experimentally challenging to uniformly fill larger microwells with well-packed cell clusters. The improved fusion of vCTBs in small micropatterned islands strongly suggests that the micropatterned culture platform may be fundamentally applicable to studies of fusion regardless of cell type and source.

DISCUSSION

Biochemical and pharmacological factors are well-established triggers and inhibitors of STB formation. However, it remains challenging to completely fuse villous cytotrophoblasts into a large STB using current in vitro techniques. By culturing villous trophoblasts on micropatterned adhesive islands that mimic the stresses present during budding morphogenesis of the villous tree structures observed in vivo, we (1) demonstrate that mechanically directed culture techniques can play a significant role in enhancing fusion processes; (2) reveal that control of the mechanical culture environment may be a viable strategy to manipulate fusion in vitro to study external regulators and effectors of functional phenotypes in pregnancy disorders; and (3) suggest that mechanical forces present during dynamic tissue morphogenesis play a critical role in placental cell and tissue function (Figure 6). Hence, the formation of the villous syncytial sheath occurs robustly and reliably in vivo because they form because of transient endogenous mechanical stresses present during the dynamic process of developmental placental tissue morphogenesis. This understanding simultaneously explains why developing well-fused culture models in static in vitro settings is so challenging while providing a potential path toward next-generation placental models for fundamental and applied placental studies.

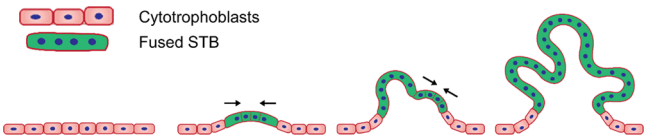

Figure 6. Proposed mechanism for in vivo formation of a completely fused syncytiotrophoblast layer around the villous tree structure in which dynamic forces generated during the budding morphogenesis process sequentially prompt fusion during morphogenesis.

Our findings strongly suggest that endogenous mechanical signals play a previously unrecognized role in placental villous trophoblast fusion. Some evidence in the literature supports this idea as generic membrane fusion has been shown to be regulated by the mechanosensor myosin II, which modulates local membrane tension to drive pore formation prior to fusion.[42] More specifically for placental trophoblasts, vCTB fusion does involve drastic perturbations of intercellular junctions and rearrangement of the internal cytoskeleton, leading to disruption and remodeling of E-cadherin and f-actin.[34] Both markers are intimately linked to mechanical forces within and around the cells[43] and are well-established players in mechanobiological processes in which cells sense and respond to mechanical stimuli.[44−46] Furthermore, these structures have a substantial impact on controlling a wide range of downstream cell configurations, phenotypes, and functions,[47−49] most notably in stem cell differentiation.[50] The drastic change in the signature of these two biomarkers strongly suggests that fusion could be regulated by mechanical or biophysical stimuli, as demonstrated in our work.

Fusion in other biological systems has recently been studied using micropatterned substrates, but with distinctly different results. Zhu et al.[33] demonstrate that breast cancer cells fuse into giant multinucleated cells in micropatterned substrates, and that biomechanical factors including reducing intracellular forces via ROCK inhibition promote and stabilize cancer cell fusion. In contrast, we show that fusion of placental villous trophoblasts is significantly inhibited by reducing intracellular tension. This indicates that the underlying fusion mechanisms between the two cell types might be fundamentally distinct, suggesting that even for superficially similar processes, the role of the tissue microenvironment is not necessarily conserved between systems.

Now that mechanical stresses induced in micropatterned cultures have been established to spatially direct and synergistically enhance villous trophoblast fusion efficiency, the underlying details of this mechanism remain to be explored. Despite careful control over micropattern size, many mechanical parameters change simultaneously in these cultures, and there likely exists a complex relationship between stress gradients, cell shape, cellular compaction, and the levels of fusion attainable in culture. Our findings are consistent with previous studies showing that cells allowed to spread freely on an unconfined substrate develop large focal adhesions and highly organized stress fibers, which decreases actin dynamics and membrane flexibility, both of which do not favor trophoblast fusion.[51] The geometrically confined culture regions used here limit cell spreading, maintaining cells in the center of the colony with sufficient mechanical tension[52] to allow fusion competency but not excessive tension that would reduce fusion efficiency. Micropatterned colonies are also expected to compact during culture due to the stress gradient generated by endogenous tension.[53] This stress gradient in circular micropatterned colonies could enhance cellular compression at the colony center, which could accelerate the fusion process. Finally, the stress gradients themselves may play a distinct role from stress magnitudes in fusion. Teasing apart these factors would be an interesting next step in better understanding fusion mechanics and dynamics.

Interestingly, the size of the syncytial patches formed in the center of smaller micropatterned islands is roughly similar to the size of the multiple separate syncytial patches found in larger micropatterns (500 μm diameter) and in unconfined conditions. Here, both BeWo cell lines and primary vCTBs demonstrate a heterogeneous and spatially unpredictable fusion pattern in unconfined culture and in large micropatterns, where syncytia are formed randomly throughout the pattern. This suggests that stochastic mechanical heterogeneity, known to arise in epithelial cell cultures,[54] may be responsible for the random formation of syncytial patches and that these patches create a fusion-suppressive field in the surrounding cells that prevents a large-scale syncytium from forming. Speculatively, this fusion-suppressive field could be driven by the observed loss of f-actin (Figure 3B) or other mechanostructural proteins that alter mechanical tension in the

DOI: 10.1021/acsami.9b19906
ACS Appl. Mater. Interfaces 2019, 11, 47810−47821

cytoskeleton, preventing the formation of pro-fusion stress gradients in the surroundings. In contrast, micropatterned cultures direct stochastically generated mechanical stress patterns to be more spatially reproducible, and sufficiently small patterns hence result in robust and reproducible fusion events.

Taken together, our results strongly suggest that appropriate design of adhesive culture patterns and the mechanical microenvironment surrounding microtissues can serve as critically important design parameters to enhance fusion in vitro. Exploring this design space will be of critical importance when developing next-generation drug screening technologies such as "organ-on-a-chip" platforms,[55] including recently developed placenta-on-a-chip model systems,[56,57] which will ultimately enhance our understanding of these complex biological systems and provide a versatile set of tools to improve disease modeling and therapeutic development strategies.

CONCLUSIONS

Despite the established role of exogenous signals in regulating fusion of villous trophoblasts into the STB layer, little is known of the role played by endogenous biophysical stresses during villous tree developmental morphogenesis in driving syncytial cell fusion. In this work, we used biomimetic micropatterning techniques to clearly demonstrate that trophoblast fusion is sensitive to mechanical conditions present during morphogenetic budding that gives rise to the placental villous tree. In the simple circular patterns tested here, fusion efficiency was enhanced by up to 3-fold, and production of the functional secreted factor β-hCG appears to be differentially regulated from the fusion process, being produced in larger quantities toward the edges of fused patches. These results suggest new avenues of research in manipulating both trophoblast fusion and syncytial patch function, a critically important next step in developing physiologically realistic in vitro drug screening and discovery platforms.

ASSOCIATED CONTENT

Supporting Information

The Supporting Information is available free of charge at https://pubs.acs.org/doi/10.1021/acsami.9b19906.

> von Mises stress and von Mises stress gradients vary in magnitude but remain similar in shape, irrespective of endogenous cell contraction; representative images of E-cadherin and nuclei from unconfined and micropatterned cultures with inhibition of mechanosensing myosin II with Blebbistatin and ROCK with Y-27632; costained fluorescent images of intracellular β-hCG, f-actin, and nuclei in micropatterns of 100 and 200 μm diameters (PDF)

AUTHOR INFORMATION

Corresponding Author

*Email: chris.moraes@mcgill.ca. Tel.: +1.514.398.4278.

ORCID

Christopher Moraes: 0000-0002-8950-2212

Author Contributions

Z.M., L.S.-F., C.V., and C.M. designed the experiment. Z.M., L.S.-F., P.K.P., and N.K. performed the experiment. R.T. performed the simulations. Z.M., L.S.-F., R.T., P.K.P., N.K., C.V., and C.M. wrote the manuscript. The final version has been approved by all authors.

Funding

This work was supported by the Fonds de Recherche du Québec (FRQ) - Nature et technologies (grant no. 205292, to C.M. and C.V.), Natural Sciences and Engineering Research Council of Canada (Discovery RGPIN-2015-05512), and the Canada Research Chair in Advanced Cellular Microenvironments to C.M. Authors gratefully acknowledge personnel funding from NSERC Postdoctoral fellowship (L.S.-F.).

Notes

The authors declare no competing financial interest.

ACKNOWLEDGMENTS

We acknowledge Pooja Patel for assistance with hydrogel ECM patterning required for traction force microscopy experiments.

REFERENCES

(1) McCarthy, F. P.; Kingdom, J. C.; Kenny, L. C.; Walsh, S. K. Animal Models of Preeclampsia; Uses and Limitations. *Placenta* **2011**, *32*, 413−419.

(2) Duley, L. The Global Impact of Pre-Eclampsia and Eclampsia. *Semin. Perinatol.* **2009**, *33*, 130−137.

(3) Law, A.; McCoy, M.; Lynen, R.; Curkendall, S. M.; Gatwood, J.; Juneau, P. L.; Landsman-Blumberg, P. The Prevalence of Complications and Healthcare Costs during Pregnancy. *J. Med. Econ.* **2015**, *18*, 533−541.

(4) Huppertz, B.; Bartz, C.; Kokozidou, M. Trophoblast Fusion: Fusogenic Proteins, Syncytins and ADAMs, and Other Prerequisites for Syncytial Fusion. *Micron* **2006**, *37*, 509−517.

(5) Vignery, A. Osteoclasts and Giant Cells: Macrophage−Macrophage Fusion Mechanism. *Int. J. Exp. Pathol.* **2000**, *81*, 291−304.

(6) Rochlin, K.; Yu, S.; Roy, S.; Baylies, M. K. Myoblast Fusion: When It Takes More to Make One. *Dev. Biol.* **2010**, *341*, 66−83.

(7) Benirschke, K.; Burton, G. J.; Baergen, R. N. Architecture of Normal Villous Trees. In *Pathology of the Human Placenta*; Benirschke, K., Burton, G. J., Baergen, R. N., Eds.; Springer Berlin Heidelberg: Berlin, Heidelberg, 2012; pp 101−144.

(8) Fuchs, R.; Ellinger, I. Endocytic and Transcytotic Processes in Villous Syncytiotrophoblast: Role in Nutrient Transport to the Human Fetus. *Traffic* **2004**, *5*, 725−738.

(9) Li, L.; Schust, D. J. Isolation, Purification and in Vitro Differentiation of Cytotrophoblast Cells from Human Term Placenta. *Reprod. Biol. Endocrinol.* **2015**, *13*, 71.

(10) Mor, G.; Aldo, P.; Alvero, A. B. The Unique Immunological and Microbial Aspects of Pregnancy. *Nat. Rev. Immunol.* **2017**, *17*, 469−482.

(11) Enders, A. C.; Blankenship, T. N. Comparative Placental Structure. *Adv. Drug Delivery Rev.* **1999**, *38*, 3−15.

(12) Black, S.; Kadyrov, M.; Kaufmann, P.; Ugele, B.; Emans, N.; Huppertz, B. Syncytial Fusion of Human Trophoblast Depends on Caspase 8. *Cell Death Differ.* **2004**, *11*, 90−98.

(13) Alsat, E.; Wyplosz, P.; Malassiné, A.; Guibourdenche, J.; Porquet, D.; Nessmann, C.; Evain-Brion, D. Hypoxia Impairs Cell Fusion and Differentiation Process in Human Cytotrophoblast, in Vitro. *J. Cell. Physiol.* **1996**, *168*, 346−353.

(14) Jansson, T.; Powell, T. L. Human Placental Transport in Altered Fetal Growth: Does the Placenta Function as a Nutrient Sensor? − A Review. *Placenta* **2006**, *27*, 91−97.

(15) Tuuli, M. G.; Longtine, M. S.; Nelson, D. M. Review: Oxygen and Trophoblast Biology − A Source of Controversy. *Placenta* **2011**, *32*, S109−S118.

(16) Lee, J.; Abdeen, A. A.; Wycislo, K. L.; Fan, T. M.; Kilian, K. A. Interfacial Geometry Dictates Cancer Cell Tumorigenicity. *Nat. Mater.* **2016**, *15*, 856−862.

DOI: 10.1021/acsami.9b19906
ACS Appl. Mater. Interfaces 2019, 11, 47810−47821

(17) Nelson, C. M.; Jean, R. P.; Tan, J. L.; Liu, W. F.; Sniadecki, N. J.; Spector, A. A.; Chen, C. S. Emergent Patterns of Growth Controlled by Multicellular Form and Mechanics. *PNAS* **2005**, *102*, 11594−11599.
(18) Lee, W.; Kalashnikov, N.; Mok, S.; Halaoui, R.; Kuzmin, E.; Putnam, A. J.; Takayama, S.; Park, M.; McCaffrey, L.; Zhao, R.; Leask, R. L.; Moraes, C. Dispersible Hydrogel Force Sensors Reveal Patterns of Solid Mechanical Stress in Multicellular Spheroid Cultures. *Nat. Commun.* **2019**, *10*, 144.
(19) Xue, X.; Sun, Y.; Resto-Irizarry, A. M.; Yuan, Y.; Yong, K. M. A.; Zheng, Y.; Weng, S.; Shao, Y.; Chai, Y.; Studer, L.; Fu, J. Mechanics-Guided Embryonic Patterning of Neuroectoderm Tissue from Human Pluripotent Stem Cells. *Nature Materials* **2018**, *17*, 633.
(20) Deglincerti, A.; Etoc, F.; Guerra, M. C.; Martyn, I.; Metzger, J.; Ruzo, A.; Simunovic, M.; Yoney, A.; Brivanlou, A. H.; Siggia, E.; Warmflash, A. Self-Organization of Human Embryonic Stem Cells on Micropatterns. *Nat. Protoc.* **2016**, *11*, 2223−2232.
(21) Humphrey, J. D.; Dufresne, E. R.; Schwartz, M. A. Mechanotransduction and Extracellular Matrix Homeostasis. *Nat. Rev. Mol. Cell Biol.* **2014**, *15*, 802−812.
(22) Nelson, C. M.; Liu, W. F.; Chen, C. S. Manipulation of Cell-Cell Adhesion Using Bowtie-Shaped Microwells. In *Adhesion Protein Protocols*; Methods in Molecular Biology™; Humana Press: 2007; pp 1−9.
(23) Moraes, C.; Kim, B. C.; Zhu, X.; Mills, K. L.; Dixon, A. R.; Thouless, M. D.; Takayama, S. Defined Topologically-Complex Protein Matrices to Manipulate Cell Shape via Three-Dimensional Fiber-like Patterns. *Lab Chip* **2014**, *14*, 2191−2201.
(24) Kliman, H. J.; Nestler, J. E.; Sermasi, E.; Sanger, J. M.; Strauss, J. F., III Purification, Characterization, and in Vitro Differentiation of Cytotrophoblasts from Human Term Placentae. *Endocrinology* **1986**, *118*, 1567−1582.
(25) Sagrillo-Fagundes, L.; Clabault, H.; Laurent, L.; Hudon-Thibeault, A.-A.; Salustiano, E. M. A.; Fortier, M.; Bienvenue-Pariseault, J.; Yen, P. W.; Sanderson, T. J.; Vaillancourt, C. Human Primary Trophoblast Cell Culture Model to Study the Protective Effects of Melatonin Against Hypoxia/Reoxygenation-Induced Disruption. *J. Visualized Exp.* **2016**, No. e54228.
(26) Clabault, H.; Laurent, L.; Sanderson, J. T.; Vaillancourt, C. Isolation and Purification of Villous Cytotrophoblast Cells from Term Human Placenta. In *Preeclampsia : Methods and Protocols*; Murthi, P., Vaillancourt, C., Eds.; Methods in Molecular Biology; Springer New York: New York, NY, 2018; pp 219−231.
(27) Rape, A. D.; Guo, W.; Wang, Y. The Regulation of Traction Force in Relation to Cell Shape and Focal Adhesions. *Biomaterials* **2011**, *32*, 2043−2051.
(28) Chandrasekaran, A.; Kouthouridis, S.; Lee, W.; Lin, N.; Ma, Z.; Turner, M. J.; Hanrahan, J. W.; Moraes, C. Magnetic Microboats for Floating, Stiffness Tunable, Air−Liquid Interface Epithelial Cultures. *Lab Chip* **2019**, *19*, 2786−2798.
(29) Tseng, Q.; Duchemin-Pelletier, E.; Deshiere, A.; Balland, M.; Guillou, H.; Filhol, O.; Théry, M. Spatial Organization of the Extracellular Matrix Regulates Cell−Cell Junction Positioning. *PNAS* **2012**, *109*, 1506−1511.
(30) Gauster, M.; Siwetz, M.; Orendi, K.; Moser, G.; Desoye, G.; Huppertz, B. Caspases Rather than Calpains Mediate Remodelling of the Fodrin Skeleton during Human Placental Trophoblast Fusion. *Cell Death Differ.* **2010**, *17*, 336−345.
(31) Brown, L. M.; Lacey, H. A.; Baker, P. N.; Crocker, I. P. E-Cadherin in the Assessment of Aberrant Placental Cytotrophoblast Turnover in Pregnancies Complicated by Pre-Eclampsia. *Histochem. Cell Biol.* **2005**, *124*, 499−506.
(32) Bushway, M. E.; Gerber, S. A.; Fenton, B. M.; Miller, R. K.; Lord, E. M.; Murphy, S. P. Morphological and Phenotypic Analyses of the Human Placenta Using Whole Mount Immunofluorescence. *Biol. Reprod.* **2014**, *90*, 110.
(33) Zhu, P.; Tseng, N.-H.; Xie, T.; Li, N.; Fitts-Sprague, I.; Peyton, S. R.; Sun, Y. Biomechanical Microenvironment Regulates Fusogenicity of Breast Cancer Cells. *ACS Biomater. Sci. Eng.* **2019**, *5*, 3817−3827.
(34) Ishikawa, A.; Omata, W.; Ackerman, W. E., IV; Takeshita, T.; Vandré, D. D.; Robinson, J. M. Cell Fusion Mediates Dramatic Alterations in the Actin Cytoskeleton, Focal Adhesions, and E-cadherin in Trophoblastic Cells. *Cytoskeleton* **2014**, *71*, 241−256.
(35) Coutifaris, C.; Kao, L. C.; Sehdev, H. M.; Chin, U.; Babalola, G. O.; Blaschuk, O. W.; Strauss, J. F., 3rd E-Cadherin Expression during the Differentiation of Human Trophoblasts. *Development* **1991**, *113*, 767−777.
(36) Adibi, J. J.; Whyatt, R. M.; Hauser, R.; Bhat, H. K.; Davis, B. J.; Calafat, A. M.; Hoepner, L. A.; Perera, F. P.; Tang, D.; Williams, P. L. Transcriptional Biomarkers of Steroidogenesis and Trophoblast Differentiation in the Placenta in Relation to Prenatal Phthalate Exposure. *Environ. Health Perspect.* **2010**, *118*, 291−296.
(37) Chen, J.; Douglas, G. C.; Thirkill, T. L.; Lohstroh, P. N.; Bielmeier, S. R.; Narotsky, M. G.; Best, D. S.; Harrison, R. A.; Natarajan, K.; Pegram, R. A.; Overstreet, J. W.; Lasley, B. L. Effect of Bromodichloromethane on Chorionic Gonadotrophin Secretion by Human Placental Trophoblast Cultures. *Toxicol. Sci.* **2003**, *76*, 75−82.
(38) Heinonen, S.; Ryynänen, M.; Kirkinen, P.; Saarikoski, S. Elevated Midtrimester Maternal Serum HCG in Chromosomally Normal Pregnancies Is Associated with Preeclampsia and Velamentous Umbilical Cord Insertion. *Am. J. Perinatol.* **1996**, *13*, 437−441.
(39) Hsu, C.-D.; Chan, D. W.; Iriye, B.; Johnson, T. R. B.; Hong, S.-F.; Repke, J. T. Elevated Serum Human Chorionic Gonadotropin as Evidence of Secretory Response in Severe Preeclampsia. *Am. J. Obstet. Gynecol.* **1994**, *170*, 1135−1138.
(40) Ashour, A. M. N.; Lieberman, E. S.; Haug, L. E. W.; Repke, J. T. The Value of Elevated Second-Trimester β-Human Chorionic Gonadotropin in Predicting Development of Preeclampsia. *Am. J. Obstet. Gynecol.* **1997**, *176*, 438−442.
(41) Delidaki, M.; Gu, M.; Hein, A.; Vatish, M.; Grammatopoulos, D. K. Interplay of CAMP and MAPK Pathways in HCG Secretion and Fusogenic Gene Expression in a Trophoblast Cell Line. *Mol. Cell. Endocrinol.* **2011**, *332*, 213−220.
(42) Kim, J. H.; Ren, Y.; Ng, W. P.; Li, S.; Son, S.; Kee, Y.-S.; Zhang, S.; Zhang, G.; Fletcher, D. A.; Robinson, D. N.; Chen, E. H. Mechanical Tension Drives Cell Membrane Fusion. *Dev. Cell* **2015**, *32*, 561−573.
(43) Moraes, C.; Sun, Y.; Simmons, C. A. (Micro)Managing the Mechanical Microenvironment. *Integr. Biol.* **2011**, *3*, 959−971.
(44) Schwarz, U. S.; Gardel, M. L. United We Stand − Integrating the Actin Cytoskeleton and Cell−Matrix Adhesions in Cellular Mechanotransduction. *J. Cell Sci.* **2012**, *125*, 3051−3060.
(45) Bays, J. L.; Campbell, H. K.; Heidema, C.; Sebbagh, M.; DeMali, K. A. Linking E-Cadherin Mechanotransduction to Cell Metabolism through Force-Mediated Activation of AMPK. *Nat. Cell Biol.* **2017**, *19*, 724−731.
(46) Harris, A. R.; Jreij, P.; Fletcher, D. A. Mechanotransduction by the Actin Cytoskeleton: Converting Mechanical Stimuli into Biochemical Signals. *Annu. Rev. Biophys.* **2018**, *47*, 617−631.
(47) Yeung, T.; Georges, P. C.; Flanagan, L. A.; Marg, B.; Ortiz, M.; Funaki, M.; Zahir, N.; Ming, W.; Weaver, V.; Janmey, P. A. Effects of Substrate Stiffness on Cell Morphology, Cytoskeletal Structure, and Adhesion. *Cell Motil.* **2005**, *60*, 24−34.
(48) Sunyer, R.; Conte, V.; Escribano, J.; Elosegui-Artola, A.; Labernadie, A.; Valon, L.; Navajas, D.; García-Aznar, J. M.; Muñoz, J. J.; Roca-Cusachs, P.; Trepat, X. Collective Cell Durotaxis Emerges from Long-Range Intercellular Force Transmission. *Science* **2016**, *353*, 1157−1161.
(49) Kong, H. J.; Liu, J.; Riddle, K.; Matsumoto, T.; Leach, K.; Mooney, D. J. Non-Viral Gene Delivery Regulated by Stiffness of Cell Adhesion Substrates. *Nat. Mater.* **2005**, *4*, 460−464.
(50) Engler, A. J.; Sen, S.; Sweeney, H. L.; Discher, D. E. Matrix Elasticity Directs Stem Cell Lineage Specification. *Cell* **2006**, *126*, 677−689.
(51) Shibukawa, Y.; Yamazaki, N.; Kumasawa, K.; Daimon, E.; Tajiri, M.; Okada, Y.; Ikawa, M.; Wada, Y.; Wang, Y.-L. Calponin 3

DOI: 10.1021/acsami.9b19906
ACS Appl. Mater. Interfaces 2019, 11, 47810−47821

Regulates Actin Cytoskeleton Rearrangement in Trophoblastic Cell Fusion. *Mol. Biol. Cell* **2010**, *21*, 3973−3984.
(52) Tan, J. L.; Tien, J.; Pirone, D. M.; Gray, D. S.; Bhadriraju, K.; Chen, C. S. Cells Lying on a Bed of Microneedles: An Approach to Isolate Mechanical Force. *PNAS* **2003**, *100*, 1484−1489.
(53) Leight, J. L.; Liu, W. F.; Chaturvedi, R. R.; Chen, S.; Yang, M. T.; Raghavan, S.; Chen, C. S. Manipulation of 3D Cluster Size and Geometry by Release from 2D Micropatterns. *Cell. Mol. Bioeng.* **2012**, *5*, 299−306.
(54) Tambe, D. T.; Hardin, C. C.; Angelini, T. E.; Rajendran, K.; Park, C. Y.; Serra-Picamal, X.; Zhou, E. H.; Zaman, M. H.; Butler, J. P.; Weitz, D. A.; Fredberg, J. J.; Trepat, X. Collective Cell Guidance by Cooperative Intercellular Forces. *Nat. Mater.* **2011**, *10*, 469−475.
(55) Moraes, C.; Mehta, G.; Lesher-Perez, S. C.; Takayama, S. Organs-on-a-Chip: A Focus on Compartmentalized Microdevices. *Ann. Biomed. Eng.* **2012**, *40*, 1211−1227.
(56) Blundell, C.; Tess, E. R.; Schanzer, A. S. R.; Coutifaris, C.; Su, E. J.; Parry, S.; Huh, D. A Microphysiological Model of the Human Placental Barrier. *Lab Chip* **2016**, *16*, 3065−3073.
(57) Blundell, C.; Yi, Y.-S.; Ma, L.; Tess, E. R.; Farrell, M. J.; Georgescu, A.; Aleksunes, L. M.; Huh, D. Placenta-on-a-Chip: Placental Drug Transport-on-a-Chip: A Microengineered In Vitro Model of Transporter-Mediated Drug Efflux in the Human Placental Barrier (Adv. Healthcare Mater. 2/2018). *Adv. Healthcare Mater.* **2018**, *7*, 1870008.

DOI: 10.1021/acsami.9b19906
ACS Appl. Mater. Interfaces 2019, 11, 47810−47821